J Biomol NMR (2007) 39:53–61
DOI 10.1007/s10858-007-9174-6

ARTICLE

Domain–domain motions in proteins from time-modulated pseudocontact shifts

X. Wang · S. Srisailam · A. A. Yee · A. Lemak · C. Arrowsmith · J. H. Prestegard · F. Tian

Received: 9 April 2007 / Accepted: 19 June 2007 / Published online: 27 July 2007

Abstract In recent years paramagnetic NMR derived structural constraints have become increasingly popular for the study of biomolecules. Some of these are based on the distance and angular dependences of pseudo contact shifts (PCSs). When modulated by internal motions PCSs also become sensitive reporters on molecular dynamics. We present here an investigation of the domain–domain motion in a two domain protein (PA0128) through time-modulation of PCSs. PA0128 is a protein of unknown function from *Pseudomonas aeruginosa* (PA) and contains a Zn^{2+} binding site in the N-terminal domain. When substituted with Co^{2+} in the binding site, several resonances from the C-terminal domain showed severe line broadening along the ^{15}N dimension. Relaxation compensated CPMG experiments revealed that the dramatic increase in the ^{15}N linewidth came from contributions of chemical exchange. Since several sites with perturbed relaxation are localized to a single β-strand region, and since extracted timescales of motion for the perturbed sites are identical, and since the magnitude of the chemical exchange contributions is consistent with PCSs, the observed rate enhancements are interpreted as the result of concerted domain motion on the timescale of a few milliseconds. Given the predictability of PCS differences and the easy interpretation of the experimental results, we suggest that these effects might be useful in the study of molecular processes occurring on the millisecond to microsecond timescale.

Keywords Chemical exchange · Domain motion · Protein dynamics · Pseudocontact shift · Structural genomics

Introduction

As structural investigations of proteins coded by newly sequenced genomes progress, instances of partially structured proteins and multiple domain proteins having flexible linkers have increased. In many cases this simply presents a challenge to structure determination, but in other cases, intramolecular motions enabled by flexible portions of a protein may be biologically significant. There are sound arguments for the importance of motions, particularly those in microsecond to millisecond range, in processes such as ligand binding, protein folding, and enzyme catalysis (Eisenmesser et al. 2005; Kovrigin and Loria 2006). These arguments certainly extend to inter-domain motions in multiple-domain proteins. Characterizing such motions in terms of both amplitude and motional time scale is a challenge that requires the identification of new and useful sources of information. Here we present one source that proves particularly useful in the investigation of inter-domain motions. It stems from the modulation of pseudocontact shifts (PCSs) by protein domain–domain motions. The motional modulations of PCSs manifest themselves as additional exchange contributions to the transverse relaxation rates of nuclear spins, and lead to a quantitative assessment of the time scale of motion.

Electronic supplementary material The online version of this article (doi:10.1007/s10858-007-9174-6) contains supplementary material, which is available to authorized users.

X. Wang · J. H. Prestegard · F. Tian (✉)
Southeast Collaboratory for Biomolecular NMR,
Complex Carbohydrate Research Center, University of Georgia,
Athens, GA 30602, USA
e-mail: ftian@ccrc.uga.edu

S. Srisailam · A. A. Yee · A. Lemak · C. Arrowsmith
Ontario Cancer Institute & Department of Medical Biophysics,
University of Toronto, Toronto, ON, Canada

The target protein, PA0128 for this study is a protein of unknown function from *Pseudomonas aeruginosa* (PA), whose structure has been determined by the Northeast Structural Genomics Consortium (NESG) (PDB: 2AKL; NESG ID: paT1). An NCBI blast search had suggested that PA0128 contained a Zn ribbon-binding motif (^{8}Cxx^{11}Cx$_{n}^{25}$Cxx^{28}C) near the N-terminus. Subsequent structure determination showed this to be part of a well-defined N-terminal domain (residues 1 to 35) that was connected by an unstructured region to a well-defined C-terminal domain (residues 50–116). Four cysteines from the ^{8}Cxx^{11}Cx$_{13}^{25}$Cxx^{28}C motif form a tetrahedral Zn^{2+}-binding site. RDC data from an aligned medium indicated the existence of significant motions between two domains (unpublished data), but further characterization of this motion is lacking. It is possible to substitute the Zn^{2+} in the binding site with Co^{2+} to produce a protein with a strongly anisotropic paramagnetic site in the N-terminus. This will aid the characterization of the molecular motion through its modulation of paramagnetic PCSs.

Molecular motions in the microsecond to millisecond range can perturb the local magnetic environments of nuclear spins and introduce time dependent resonance frequencies, resulting in increases in nuclear transverse relaxation rates. This phenomenon is often referred as relaxation enhancement by chemical exchange. NMR relaxation dispersion experiments can in principle provide detailed descriptions of these dynamic processes (Ishima and Torchia 2000; Palmer 2004). Conventionally, the ^{15}N single quantum transverse relaxation rates are measured as a function of the delay (τ_{cp}) between π pulses in the Carr–Purcell–Meiboom–Gill (CPMG) sequences, or as a function of the radiofrequency spin-lock amplitude in a HSQC experiment. In CPMG related experiments, the difference between the measurement at a particular τ_{cp} and the relaxation rate in the fast pulsing limit represents the contribution from chemical exchange. The repetition rate of π pulses in the CPMG sequence, or the strength of the spin-lock field needed to eliminate the exchange contributions, defines the time scale of the molecular motion. Recently, the relaxation rates of multiple quantum coherences have also emerged as a sensitive probe for the study of correlated motions and the contributions of minor conformations in proteins (Dittmer and Bodenhausen 2004; Fruh et al. 2001; Kloiber and Konrat 2000; Korzhnev et al. 2004; Lundstrom et al. 2005; Majumdar and Ghose 2004). However, in virtually all of these applications, the origin of chemical shift modulation has been very short range (for example, local conformational change, titration of proximate charged groups, or movement of adjacent aromatic rings). Moreover, molecular motions may not result in chemical shift changes, making motion at certain sites "invisible" to relaxation dispersion experiments. Consequently, multiple relaxation rates involving several nuclei are usually measured in order to accurately characterize a dynamic process (Korzhnev et al. 2005; Korzhnev et al. 2004). The situation with paramagnetic perturbations is different.

In recent years paramagnetic NMR derived structural constraints have been demonstrated to provide complementary information to classic diamagnetic NOEs and torsion angle constraints in the structure determination of biomolecules (Bertini et al. 2002b; Hansen et al. 2003; Tolman et al. 1995). Constraints obtained from PCSs, paramagnetic relaxation enhancements (PREs), residual dipolar couplings (RDCs) and cross-correlated relaxation between Curie–spin and dipole–dipole interactions produce long-range structural information, which are difficult to obtain in conventional NMR experiments. In combination with NOE derived constraints they can improve both the quality of the structures and the efficiency of structure determinations (Bertini et al. 2001a; Bertini et al. 2002a; Pintacuda et al. 2004a; Prestegard et al. 2004). In addition, PREs and RDCs have shed new light on intermolecular interactions and molecular dynamics (Bax and Grishaev 2005; Bertini et al. 2004; Bouvignies et al. 2005; Fischer et al. 1999; Iwahara and Clore 2006; Tang et al. 2006; Tolman et al. 1997; Volkov et al. 2006).

PCSs originate from the dipolar interaction between the nuclear spin and the average induced magnetic moment of electrons (Bertini et al. 2001c). For metals with a high magnetic susceptibility anisotropy such as Co^{2+}, an orientationally dependent induced moment will arise in the presence of a magnetic field. The effect of this moment on the field seen by nearby spins does not average to zero and PCSs result. PCSs depend on the distance between the paramagnetic center and the nuclear spin as well as the orientation of the vector connecting them to the susceptibility tensor as described by the Eq. (1)

$$\delta^{\mathrm{pcs}} = \frac{1}{12\pi r^3}\left[\Delta\chi_{\mathrm{ax}}(3\cos^2\theta - 1) + \frac{3}{2}\Delta\chi_{\mathrm{rh}}\sin^2\theta\cos 2\varphi\right] \quad (1)$$

where $\Delta\chi_{ax}$ and $\Delta\chi_{rh}$ are the axial and the rhombic anisotropies of the magnetic susceptibility tensor, and θ and φ are the polar coordinates of the nuclear spin with respect to the principal axes of the magnetic susceptibility tensor. Like NOEs, PCSs are distance dependent, but affect nuclear spins over a relatively long range because of their $1/r^3$ as opposed to $1/r^6$ dependence. When a spin of interest moves between two or more positions, PCSs will, in general, be different at each position. Numerical simulations suggest the differences, particularly at high field, could be significant even for spins 20 Å distant. Although PCSs do not depend on the strength of the magnetic field on the ppm

scale, they increase linearly with field strength on the Hz scale, and it is chemical shift modulation on the Hz scale that contributes to the decay of the transverse magnetization when the exchange process is in the microsecond to millisecond range.

Paramagnetic centers exist natively in paramagnetic metalloproteins, and can be introduced artificially into other proteins with the addition of metal-binding tags (Dvoretsky et al. 2002; Gaponenko et al. 2002; Ikegami et al. 2004; Jensen et al. 2004; Ma and Led 2000; Pintacuda et al. 2004b; Wohnert et al. 2003). In the present study we introduced a paramagnetic center, Co^{2+}, into PA0128 by substitution in a site normally occupied by Zn^{2+}. ^{15}N single quantum relaxation rates were measured with relaxation-compensated CPMG sequences for both Zn^{2+} and Co^{2+} forms of the protein (Loria et al. 1999). We found that for a portion of the C-terminal domain the magnetization decay rates show pronounced dependence on delays between π pulses in the Co^{2+} form but not in the Zn^{2+} form. We interpret the exchange contributions seen in the Co^{2+} form as arising from time-dependent modulations of the PCSs by domain–domain motions on the millisecond time scale.

Materials and methods

E. coli strain BL21-(Gold DE3) encoding the PA0128 clone were grown in 1 l of 2X M9 minimal medium containing $^{15}NH_4Cl$ as the sole nitrogen source supplemented with thiamine, and biotin only. The cells were grown at 37°C to an OD_{600} of 1.0, the culture was then divided into 2 flasks. One flask was supplemented with $ZnSO_4$ to a final concentration of 20 μM, the other flask was supplemented with $CoCl_2$ to a final concentration of 20 μM. Protein expression was induced with 1 mM isopropyl β-D-thiogalactoside and the temperature was reduced to 15°C. The cells were allowed to grow overnight before harvesting. The PA0128 proteins were purified using Ni-NTA affinity chromatography. All buffers used in purification of the zinc and cobalt versions of PA0128 contained 10 μM of either $ZnSO_4$ or $CoCl_2$, respectively. The final NMR buffer was 10 mM sodium phosphate, 450 mM NaCl, 10 mM DTT, pH 6.5, 0.01% NaN3, 1 mM benzamidine, 1x protease inhibitor mixture (Roche) and 10 μM of either $ZnSO_4$ or $CoCl_2$.

All NMR data were recorded at 25°C on either 14.1 or 21.1 T instruments (INOVA 600 or 900) with room temperature probes, using a sample of the Zn^{2+} form of PA0128 at 0.25 mM and a sample of the Co^{2+} form of PA0128 at 0.4 mM. The ^{15}N R_2 relaxation data were acquired using the gNhsqc pulse sequence from BioPack (Varian Inc.) with a variable delay (τ) before ^{15}N evolution. 683 and 128 complex points were obtained along the direct and indirect dimensions, respectively, at a series of τ values of 10, 30, 50, 70, 90, 110 ms. FIDs were apodized with a standard cosine function in both dimensions and zero filled to 1024 t2 points and 256 t1 points before applying a Fourier transform. The R_2 rate constants were calculated with the rate analysis function panel in NMRView (version 5.0.4), which implements a two-parameter exponential fit using the Levenberg–Marquardt method.

The ^{15}N relaxation dispersion data were measured at 21.1 T at τ_{cp} delays of 1, 5, 10 and 64.5 ms for the Zn^{2+} loaded form, and at τ_{cp} delays of 1, 5, 10 and 21.5 ms for the Co^{2+} loaded form. For short τ_{cp} values of 1, 5 and 10 ms the relaxation-compensated CPMG pulse sequence was employed (Loria et al. 1999). For long τ_{cp} values of 21.5 and 64.5 ms the Hahn-echo sequence was used (Millet et al. 2000). Two time points were recorded to determine the relaxation rate constants for each τ_{cp} delay. One point was at zero. Another point, which was duplicated three times, was at 20 and 60 ms for Co^{2+} and Zn^{2+} bound PA0128, respectively. In total 48 2D spectra were acquired with (98 × 1024) complex points and spectral widths of 2800 and 14524 Hz along indirect and direct dimensions. 32 scans per increment were taken for each indirect point at a 3 s recycle delay.

Relaxation dispersion curves for $R_2(1/\tau_{cp})$ were fit to a fast-limit equation for two exchanging sites:

$$R_2(1/\tau_{cp}) = R_2(1/\tau_{cp} \rightarrow \infty) + \Phi_{ex}\tau_{ex}[1 - (2\tau_{ex}/\tau_{cp})\tanh(\tau_{cp}/2\tau_{ex})] \quad (2)$$

where $R_2(1/\tau_{cp} \rightarrow \infty)$ is the averaged relaxation rate constant for in-phase and antiphase ^{15}N magnetization; $\Phi_{ex} = (\varpi_1 - \varpi_2)^2 p_1 p_2$; ϖ_i and p_i are the Larmor frequencies and populations for the nuclear spin at site i; τ_{ex} is the lifetime for the exchange process; and τ_{cp} is the delay between pulses in the spin-echo pulse train.

Results and discussion

Substitution of Zn^{2+} with Co^{2+} in the binding site of PA0128 leads to significant resonance broadening in HSQC spectra (Fig. 1). At magnetic fields employed in this study both dipole–dipole and Curie–dipole spin relaxation mechanisms may be active. Co^{2+} atoms coordinated with four sulfur ligands are likely to be in a high-spin state with an electron spin relaxation time on the order of 10^{-11} s (Bertini et al. 2001c). The rotational correlation time of PA0128 is estimated to be about 5 ns from amide nitrogen T_1s and T_2s of the Zn^{2+} form. Using these correlation times, the ratio of the relaxation contribution from the Curie–nuclear spin interaction to the contribution from the

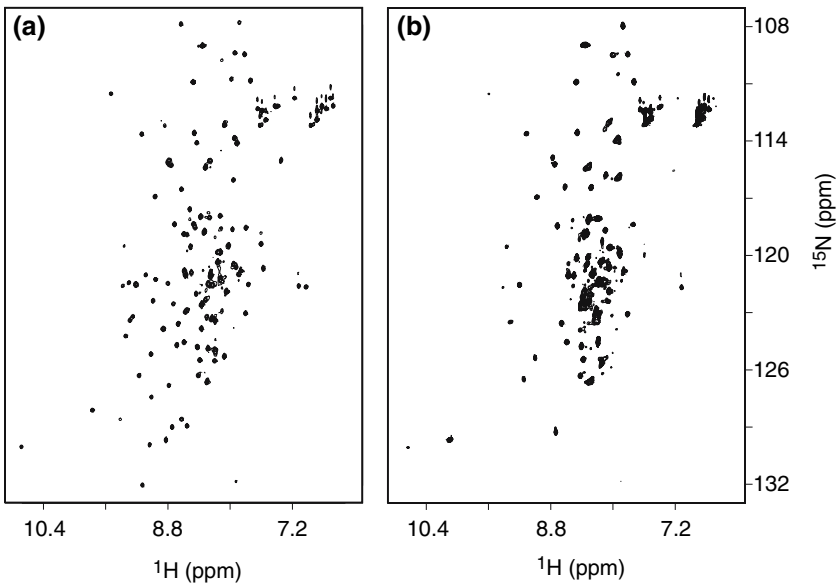

Fig. 1 2D ^{15}N-^{1}H HSQC spectra recorded on Zn^{2+} (left) and Co^{2+} (right) loaded PA0128 at 900 MHz

electron spin–nuclear spin interaction is estimated to be 3 and 1.4 at magnetic fields of 21.1 and 14.1 T, respectively (Mispelter et al. 1993). Regardless of the mechanism, 24 out of 30 resonances from the N-terminal domain observable in the Zn^{2+} sample were not detected in the HSQC spectrum of the Co^{2+} sample. These correspond to sites that are less than 15 Å away from the metal. The remaining six resonances are unfortunately either overlapped with other resonances, or shifted too far from positions in the Zn^{2+} form to allow unambiguous assignments. In the future, direct detection of ^{13}C or ^{15}N nuclei may be utilized to observe and assign N-terminal sites (Bermel et al. 2006), which will allow the determination of the magnetic susceptibility tensor and the study of the amplitudes of domain–domain motions with RDCs (Bertini et al. 2004; Fischer et al. 1999; Rodriguez-Castaneda et al. 2006). However, our focus here is on the C-terminal domain. Resonances from the C-terminal domain and the linker in the Co^{2+} sample are not extensively broadened and are only slightly shifted. About half of them can be identified based on the assignments for the Zn^{2+} form. The observed PCSs are relatively small for ^{15}N, ranging from –0.421 to 0.268 ppm and are even smaller for ^{1}H, ranging from –0.068 to 0.063 ppm. For observable resonances, the PCSs for ^{15}N and ^{1}H are expected to have similar values on the ppm scale (Bertini et al. 2001b). The unusually small ^{1}H shift in the current study is believed due to the domain–domain motion having effects in different motional regimes for ^{1}H and ^{15}N nuclear spins as explained further below.

Comparing HSQC spectra collected at 600 and 900 MHz, several resonances exhibited severe line broadening in data recorded at 900 MHz on Co^{2+} loaded PA0128, while little difference was observed for these resonances in data recorded on the Zn^{2+} loaded form. This broadening appears to occur in both ^{15}N and ^{1}H dimensions. An example is shown in Fig. 2. Spectra (a) and (c) were recorded on the Zn^{2+} form, and spectra (b) and (d) were recorded on the Co^{2+} form. Resonances T39 and I85 are significantly broader and weaker at 900 (Fig. 2d) than at 600 MHz (Fig. 2b), while their linewidths are very similar in spectra Fig. 2a and Fig. 2c. Although increases in proton linewidths might be explained by contributions from the field squared dependent Curie–spin relaxation, significant increases in ^{15}N linewidths were unexpected. Because both the dipolar and Curie paramagnetic broadenings depend on the square of the gyromagnetic ratio of the nuclear spins (Bertini et al. 2001c), the paramagnetic relaxation enhancements are expected to be ~100 times more effective for ^{1}H than for ^{15}N spins. If the observed dramatic increases in the ^{15}N linewidths solely came from paramagnetic relaxation enhancements, the proton lines would be broadened beyond detection. Thus, the resonance broadening along ^{15}N dimension must come from other sources.

The observations presented in Fig. 2 are better elucidated with more quantitative measurements based on CPMG experiments. The ^{15}N transverse relaxation rates were first measured using a very short delay, 1.25 ms between π pulses for both Co^{2+} and Zn^{2+} loaded PA0128. Under these conditions, exchange contributions from slow motions to R_2 should be minimal. The experimental data are plotted in Fig. 3. The average R_2 for the Zn^{2+} form at 600 MHz is 8.3 s^{-1}; this agrees with the expected rate for a protein of this size. The average values for the Co^{2+} form at 600 and 900 MHz are 15.4 and 17.3 s^{-1}, respectively. Ratios of amide nitrogen R_2s at 900 to those at 600 MHz for the Co^{2+} form ranged only from 1.01 to 1.26. This is

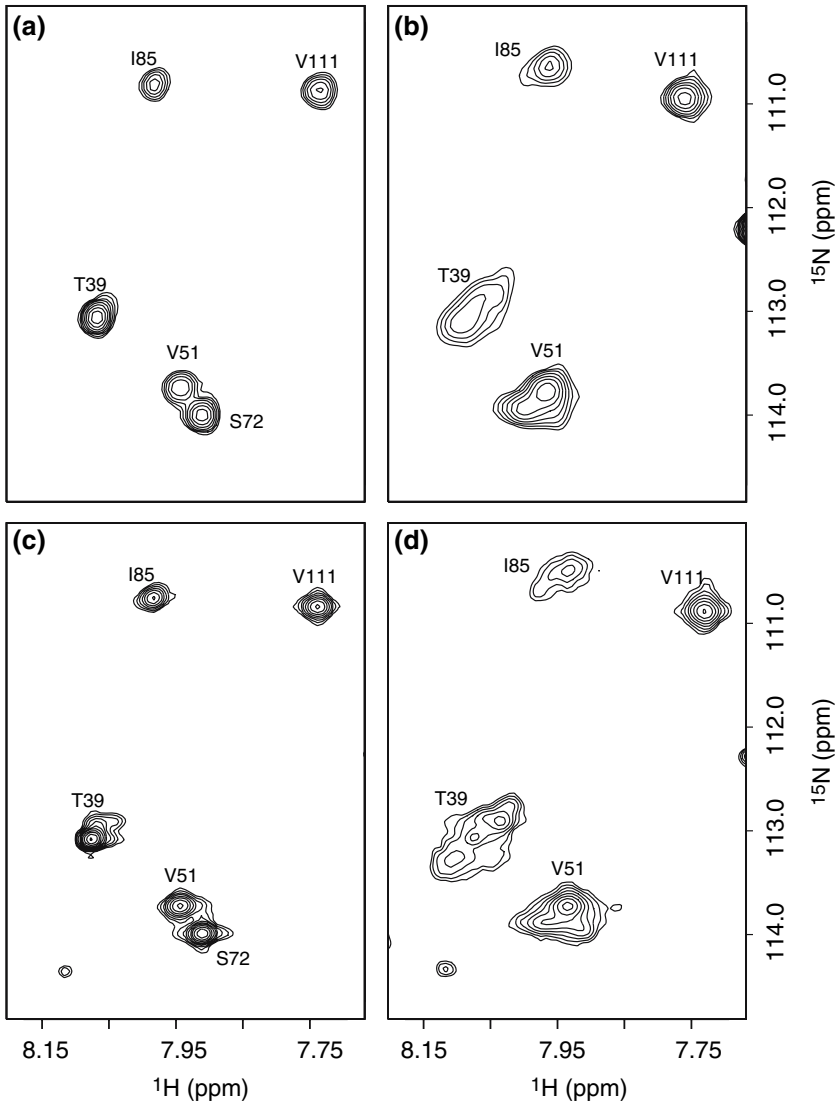

Fig. 2 Expanded regions of 2D ^{15}N-^{1}H HSQC spectra recorded on Zn^{2+} (left) and Co^{2+} (right) loaded PA0128. Spectra (**a**) and (**b**) were recorded at 600 MHz; Spectra (**c**) and (**d**) were recorded at 900 MHz. Excess line broadening along ^{15}N dimension was observed on the Co^{2+} loaded sample at 900 MHz

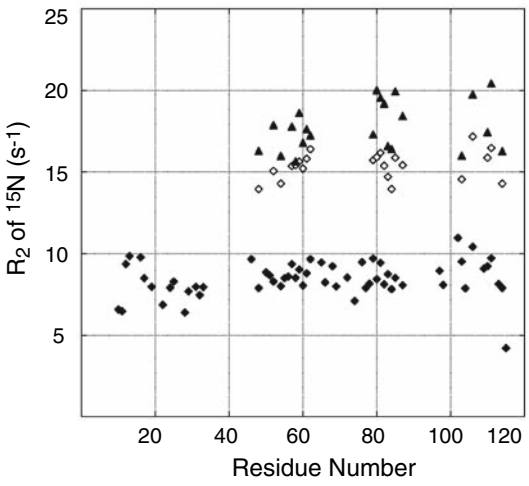

Fig. 3 ^{15}N transverse relaxation rates. ◆: Zn^{2+} loaded PA0128 at 600 MHz; ◇: Co^{2+} loaded PA0128 at 600 MHz; ▲: Co^{2+} loaded PA0128 at 900 MHz

consistent with Curie–spin paramagnetic relaxation making little contribution to the ^{15}N R_2s. The small field dependence is consistent with larger ^{15}N CSA contributions to the transverse relaxation at higher field. However, there is a rather uniform enhancement of ^{15}N R_2s in comparing Co^{2+} to Zn^{2+} data at 600 MHz. This is unexpected (Fig. 3), because both dipole–dipole and Curie–dipole paramagnetic relaxation enhancements should have little effect on the R_2s of amide nitrogen for observable resonances. One possible contribution to this more global R_2 difference between the Co^{2+} and Zn^{2+} forms could originate from delocalization of unpaired electron spin density onto the $2p_z$ orbitals of the ^{15}N nuclei; this mechanism, which decays more slowly with distance has previously been highlighted in a study of the paramagnetic longitudinal rates of heteronuclei (Ma et al. 2000; Mispelter et al. 1993). However, even if this is the origin, the measured ^{15}N R_2s for residue T85, 15.9 and 19.9 s^{-1} at 600 and 900 MHz,

respectively do not explain the pronounced field dependence of the resonance linewidth. Therefore, other mechanisms such as exchange broadening are pursued. Broadenings from these mechanisms have recently been shown to be very sensitive to minor populations in exchanging systems (Iwahara and Clore 2006; Korzhnev et al. 2004) and may offer the sensitivity to transient domain contacts that we seek. Below we investigate possible chemical exchange contributions to the resonance linewidths.

The ^{15}N transverse relaxation rates, $R_2(\tau_{cp})$ were measured as a function of delays between π pulses with the relaxation-compensated CPMG sequences (Loria et al. 1999; Millet et al. 2000). These experiments explicitly average the evolution of the ^{15}N transverse magnetizations between in-phase and anti-phase coherences, allowing measurements of exchange processes over a broad time scale. Figure 4a shows the differences, $\Delta R_2(\tau_{cp})$, in the measured $R_2(\tau_{cp})$ values with τ_{cp}s of 1 and 5 ms as well as the differences with τ_{cp}s of 1 and 64.5 ms for the Zn^{2+} loaded form. The experimental uncertainty was ± 1.5 s^{-1}, which included systematic errors associated with measurements using two separate sequences, but the relatively large errors were mainly due to the sensitivity limitations. Assuming the chemical exchange contributions were eliminated at a τ_{cp} of 1 ms, $\Delta R_2(\tau_{cp})$ represents their contributions to the relaxation decays. For most backbone ^{15}N resonances in the Zn^{2+} bound form of PA0128, $\Delta R_2(\tau_{cp})$s were within the experimental error. A few residues including residues 4 at the beginning of the N-terminus, residues 13 and 65 from the loop region, and residues 16, 17, 31, 68, 69, 102, 103 and 110 at the beginning or end of an α-helix or β-sheet, showed some exchange broadening (Fig. 4a). However, much larger differences, $\Delta R_2(\tau_{cp})$ in the measured $R_2(\tau_{cp})$ values were observed with τ_{cp}s of 1, 5 and 21.5 ms on the Co^{2+} form (Fig. 4b). The experimental uncertainties here were ± 2.0 s^{-1}. Observable resonances from residues 79 to 110 all showed significant differences except for residue 83. Residue 85 exhibited the largest difference. These are clearly indicative of chemical exchange contributions.

The relaxation dispersion curves for residues 80, 81, 84 and 85 from the Co^{2+} loaded sample are plotted in Fig. 5. For comparison, the dispersion curves for these residues from the Zn^{2+} sample are also plotted. The exact form of the relaxation dispersion curves depends on a model for the motion that modulates chemical shifts. It is appropriate to start with one of the simplest models, a two state model. Data from the Co^{2+} loaded sample were, therefore, fit to Eq. 2 (see methods section) to quantitatively extract exchange parameters. The fitting results are listed in Table 1. Interestingly, the lifetime of the exchange for all sites falls on a time scale of a few milliseconds, suggesting the

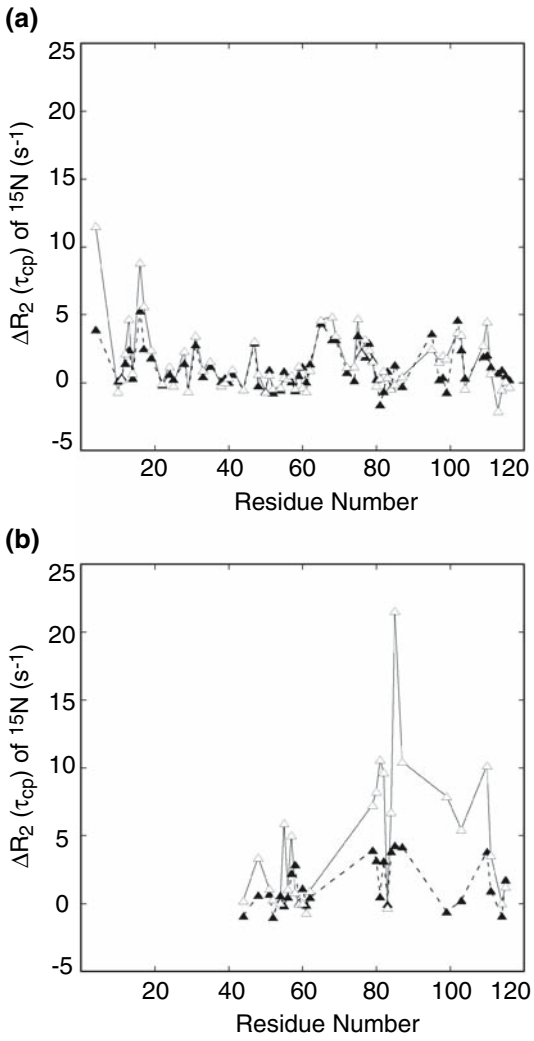

Fig. 4 Differences in the ^{15}N transverse relaxation rates measured at several τ_{cp} values, $\Delta R_2(\tau_{cp})$, are plotted against the residue number. (**a**) Zn^{2+} loaded PA0128 at 900 MHz. ▲: $\Delta R_2(\tau_{cp}) = R_2(5\text{ ms}) - R_2(1\text{ ms})$; △: $\Delta R_2(\tau_{cp}) = R_2(64.5\text{ ms}) - R_2(1\text{ ms})$. (**b**) Co^{2+} loaded PA0218 at 900 MHz. ▲: $\Delta R_2(\tau_{cp}) = R_2(5\text{ ms}) - R_2(1\text{ ms})$; △: $\Delta R_2(\tau_{cp}) = R_2(21.5\text{ ms}) - R_2(1\text{ ms})$

effects come from a single correlated motion. Modulation of the metal g-tensor by slow conformational dynamics at the metal binding site (Clore et al. 1991) can be discounted because relaxation dispersion data for three observed cysteines from the Zn^{2+} binding site do not indicate the existence of such slow conformational exchange (residue 11, 25 and 28 in Table S1). Modulation could also be caused by the Co^{2+} exchanging between bound and free states, but this is unlikely for PA0128. The Co^{2+} affinity is quite high since storage in the presence of 10 μM Co^{2+} did not reduce the bound metal content, and in all acquired HSQC spectra, there were few, if any, resonances which correspond to the unloaded form of PA0128. We therefore prefer a model in which inter-domain motion is the source of modulation.

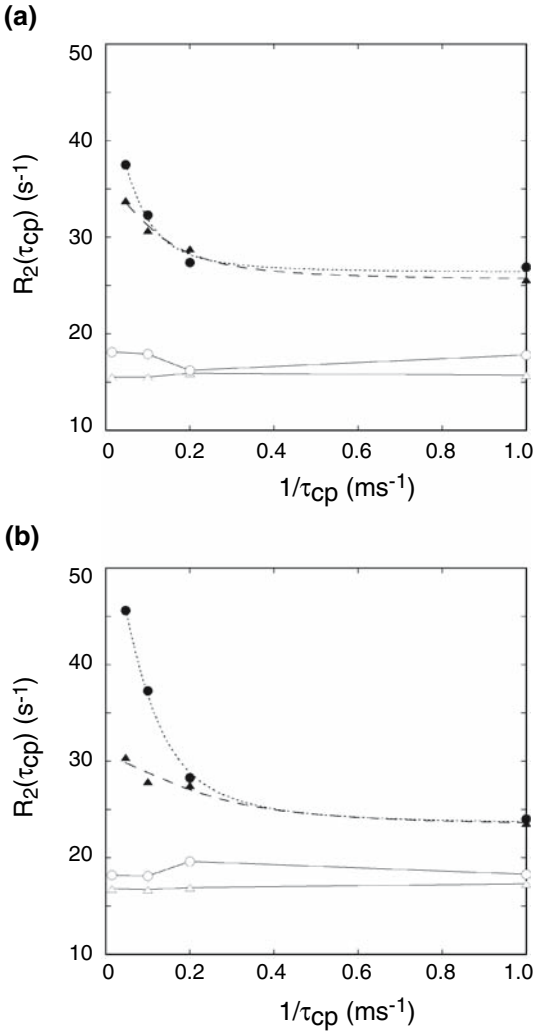

Fig. 5 Relaxation dispersion curves for PA0128 at 900 MHz. Unfilled symbols: Zn^{2+} form; filled symbols: Co^{2+} form. (**a**) triangle: T80; circle: K81. (**b**) triangle: N84; circle: I85. For the Co^{2+} form, dashed lines represent the fits to the experimental data points. The fitting results are given in Table 1. For the Zn^{2+} form, solid lines are drawn along experimental data points to improve visualization

Table 1 Relaxation dispersion parameters for Co^{2+} bound PA0128

Residue	τ_{ex} (ms)	$\Phi_{ex}\tau_{ex}$ (s^{-1})	$R_2(1/\tau_{cp} \rightarrow \infty)$ (s^{-1})
T80	2.28 ± 0.65	10.2 ± 1.5	25.6 ± 0.8
K81	4.28 ± 1.44	18.6 ± 4.2	26.4 ± 1.0
V82	6.20 ± 6.19	19.4 ± 17.9	26.8 ± 1.5
N84	1.27 ± 0.79	7.5 ± 1.9	23.3 ± 1.4
I85	3.11 ± 0.34	31.4 ± 1.9	23.5 ± 0.8

In Fig. 6b, residues with and without exchange contributions in the Co^{2+} form are colored in red and green, respectively. Interestingly, residues not exhibiting exchange contributions form a continuous surface at one

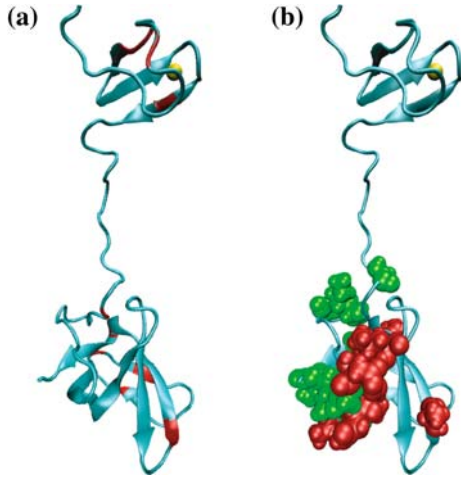

Fig. 6 Ribbon representations of the NMR solution structure of PA0128. (**a**) Residues showing exchange contributions in the Zn^{2+} form are colored in red. (**b**) Residues with and without exchange contributions in the Co^{2+} form are colored in red and green, respectively. The K83 sidechain was removed for visualization

side of the C-terminus, while the assigned residues from the remaining C-terminal domain all show exchange contribution except one, residue 83. Residues 80 to 87 are localized to a single β-strand region. Therefore, we propose the exchange contributions come from a domain motion that samples a range of more extended conformers, but includes sampling of a conformer that has close contacts between the N-terminal domain and this beta strand. Moreover, this domain–domain motion is on the time scale of a few milliseconds. We propose that it is this motion that produces time-modulations of PCSs which, like normal chemical exchange, introduces the observed resonance broadenings. The two-state model is an over simplification for this particular exchange process, but the relatively steep distance dependence of the PCSs would make shifts for all extended conformations very similar, and the localization of perturbed resonances would suggest a single, or small number of, preferred close-contact states.

The lack of observed resonances from the N-terminal domain prevented us from determining the magnetic susceptibility tensor of the Co^{2+} site, and from quantitatively analyzing the variations in PCSs. However, in two previous studies, the axial anisotropies of the susceptibility tensor for Co^{2+} in pseudotetrahedral binding sites were reported to be -3.2×10^{-32} and -4.8×10^{-32} m^3 (Bertini et al. 1991; Harper et al. 1993). Taking the average value of -4.0×10^{-32} m^3 and assuming the magnetic susceptibility tensor is axial symmetric, a nuclear spin at a single close approach site 18 Å removed along the axial direction would have a PCS of 0.36 ppm. If the second site is taken to represent a set of conformers with larger distances (≥28 Å) along the axial direction, or a set of conformers that are 22 Å away

from Co^{2+} but 35° off the tensor axial direction, the PCS would be small (≤0.1 ppm). This PCS difference can result in significant exchange contributions. Assuming a 3 ms exchange lifetime and populations of 20% and 80% at two sites, a 0.26 ppm shift difference would have an exchange contribution of 10.3 s^{-1} to the ^{15}N transverse relaxation rate at 900 MHz. This is in line with our observations and provides support for our interpretation.

The exchange contribution to ^{1}H transverse relaxation can also be estimated from above exchange parameters. Domain–domain motion on the time scale of 3 ms is in the intermediate to slow range on the ^{1}H chemical shift time scale for sites having the ^{1}H PCS differences larger than 0.2 ppm. For those resonances, the observed proton chemical shifts correspond to that expected for more highly populated states where two domains are well separated in extended conformers. Consequently, much smaller ^{1}H PCSs are detected and are different from values measured along ^{15}N dimension. Also in this regime, the exchange contribution becomes less dependent on the magnetic field, and does not show the quadratic dependence seen for fast exchange (Millet et al. 2000). In fact, for very slow exchange, it is independent of the field strength. This explains the observation that the proton linewidths only increase modestly for resonances that showed significant exchange contributions along the ^{15}N dimension at 900 MHz.

Thus, for cases where exchanges remain in the rapid regime, enhanced transverse relaxation by time-modulated PCSs provides new opportunities for the study of molecular structure and dynamics. PCS differences resulting from molecular motion are predictable, making experimental results more amenable to interpretation. Through their effects on spin relaxation they are sensitive probes of transient contacts between remote parts of biomolecules. These contacts may not lead to specific models but can be very useful in screening sets of hypothesized structures. Their sensitivity to the time scale of the molecular motion and their predictable geometric dependence might allow studies of microsecond to millisecond correlated motions which have been difficult to investigate with more traditional spin relaxation studies.

Acknowledgement This work is supported by NIH grants GM074958, GM33225 and the Ontario Research and Development Fund. We thank professor Mark Rance at University of Cincinnati for helpful discussions.

Reference

Bax A, Grishaev A (2005) Weak alignment NMR: a hawk-eyed view of biomolecular structure. Curr Opin Struct Biol 15:563–570

Bermel W, Bertini I, Felli IC, Piccioli M, Pierattelli R (2006) ^{13}C-detetced protonless NMR spectroscopy of proteins in solution. Prog Nucl Magn Reson Spectrosc 48:25–45

Bertini I, Bianco CD, Gelis I, Katsaros N, Luchinat C, Parigi G, Peana M, Provenzani A, Zoroddu MA (2004) Experimentally exploring the conformational space sampled by domain reorientation in calmodulin. Proc Natl Acad Sci USA 101:6841–6846

Bertini I, Donaire A, Jimenez B, Luchinat C, Parigi G, Piccioli M, Poggi L (2001a) Paramagnetism-based versus classical constraints: An analysis of the solution structure of Ca Ln calbindin D_{9k}. J Biomol NMR 21:85–98

Bertini I, Janik MBL, Lee YM, Luchinat C, Rosato A (2001b) Magnetic susceptibility tensor anisotropies for a lanthanide ion series in a fixed protein matrix. J Am Chem Soc 123:4181–4188

Bertini I, Longinetti M, Luchinat C, Parigi G, Sgheri L (2002a) Efficiency of paramagnetism-based constraints to determine the spatial arrangement of α-helical secondary structure elements. J Biomol NMR 22:123–136

Bertini I, Luchinat C, Parigi G (2001c) Solution NMR of paramagnetic molecules. Elsevier, Amsterdam

Bertini I, Luchinat C, Parigi G (2002b) Paramagnetic constraints: an aid for quick structure determination of paramagnetic metalloproteins. Concepts Magn Reson 14:259–286

Bertini I, Luchinat C, Piccioli M, Oliver MV, Viezzoli MS (1991) ^{1}H NMR investigation of reduced copper-cobalt superoxide dismutase. Eur Biophys J 20:269–279

Bouvignies G, Bernado P, Meier S, Cho K, Grzesiek S, Bruschweiler R, Blackkedge M (2005) Identification of slow correlated motions in proteins using residual dipolar coupling and hydrogen-bond scalar couplings. Proc Natl Acad Sci USA 102:13885–13890

Clore GM, Omichinski JG, Gronenborn AM (1991) Slow conformational dynamics at the metal coordination site of a zinc finger. J Am Chem Soc 113:4350–4351

Dittmer J, Bodenhausen G (2004) Evidence for slow motion in proteins by multiple refocusing of heteromuclear nitrogen/proton multiple quantum coherences in NMR. J Am Chem Soc 126:1314–1315

Dvoretsky A, Gaponenko V, Rosevear PR (2002) Derivation of structural restraints using thiol-reactive chelator. FEBS Lett 528:189–192

Eisenmesser EZ, Millet O, Labeikovsky W, Korzhnev DM, Wolf-watz M, Bosco DA, Skalicky JJ, Kay LE, Kern D (2005) Intrinsic dynamics of an enzyme underlies catalysis. Nature 438:117–121

Fischer MWF, Losonczi JA, Weaver JL, Prestegard JH (1999) Domain orientation and dynamics in multidomain proteins from residual dipolar couplings. Biochemistry 38:9013–9022

Fruh D, Tolman JR, Bodenhausen G, Zwahlen C (2001) Cross-correlated chemical shift modulation: a signature of slow internal motions in proteins. J Am Chem Soc 123:4810–4816

Gaponenko V, Altieri AS, Li J, Byrd RA (2002) Breaking symmetry in the structure determination of (large) symmetric protein dimers. J Biomol NMR 24:143–148

Hansen DF, Hass MAS, Christensen HM, Ulstrup J, Led JJ (2003) Detection of short-lived transient protein-protein interactions by intermolecular nuclear paramagnetic relaxation: Plastocyanin from *Anabaena variabilis*. J Am Chem Soc 125:6858–6859

Harper LV, Amann BT, Vinson VK, Berg JM (1993) NMR studies of a cobalt-substituted zinc finger peptide. J Am Chem Soc 115:2577–2580

Ikegami T, Verdier L, Sakhaii P, Grimme S, Pescatore B, Saxena K, Fiebig KM, Griesinger C (2004) Novel techniques for weak alignment of proteins in solution using chemical tags coordinating lanthanide ions. J Biomol NMR 29:339–349

Ishima R, Torchia DA (2000) Protein dynamics from NMR. Nat Struct Biol 7:740–743

Iwahara J, Clore GM (2006) Detecting transient intermediates in macromolecular binding by paramagnetic NMR. Nature 440:1227–1230

Jensen MR, Lauritzen C, Dahl SW, Pedersen J, Led JJ (2004) Binding ability of a HHP-taged protein toward Ni^{2+} studied by paramagnetic NMR relaxaton: The possibility of obtaining long-range structure information. J Biomol NMR 29:175–185

Kloiber K, Konrat R (2000) Differential multiple-quantum relaxation arising from cross-correlated time-modulation of isotropic chemical shifts. J Biomol NMR 18:13–42

Korzhnev DM, Neudecker P, Mittermaier A, Orekhov VY, Kay LE (2005) Multiple-site exchange in proteins studied with a suite of six NMR relaxation dispersion experiments: An application to the foldng of a Fyn SH3 domain mutant. J Am Chem Soc 127:15602–15611

Korzhnev DM, Salvatella X, Vendruscolo M, Di Nardo AA, Davidson AR, Dobson CM, Kay LE (2004) Low-populated folding intermediates of Fyn SH3 characterized by relaxation dispersion NMR. Nature 430:586–590

Kovrigin EL, Loria JP (2006) Characterization of the transition state of functional enzyme dynamics. J Am Chem Soc 128:7724–7725

Loria JP, Rance M, Palmer AG (1999) A relaxation-compensated Carr-Purcell-Meiboom-Gill sequence for characterizing chemical exchange by NMR spectroscopy. J Am Chem Soc 121:2331–2332

Lundstrom P, Mulder FAA, Akke M (2005) Correlated dynamics of consecutive residues reveal transient and cooperative unfolding of secondary structure in proteins. Proc Natl Acad Sci USA 102:16984–16989

Ma LX, Jorgensen A-MM, Sorensen GO, Ulstrup J, Led JJ (2000) Elucidation of the paramagnetic R_1 relaxation of heteronuclei and protons in Cu(II) plastocyanin from *Anabaena variabilis*. J Am Chem Soc 122:9473–9485

Ma LX, Led JJ (2000) Determination by high field NMR spectroscopy of the longitudinal electron relaxation rate in Cu(II) plastocyanin form Anabaena variabilis. J Am Chem Soc 122:7823–7824

Majumdar A, Ghose R (2004) Probing slow backbone dynamics in proteins using TROSY-based experiments to detect cross-correlated time-modulation of isotropic chemical shifts. J Biomol NMR 28:213–227

Millet O, Loria JP, Kroenke CD, Pons M, Palmer AG (2000) The static magnetic field dependence of chemical exchange linebroadening defines the NMR chemical shift time scale. J Am Chem Soc 122:2867–2877

Mispelter J, Momenteau M, Lhoste J-M (1993) Heteronuclear magnetic resonance applications to biological and related paramagnetic molecules. In: Berliner LJ, Reuben J (eds) Biological magnetic resonance: NMR of paramagnetic molecules, vol 12. Plenum Press, New York, pp 299–355

Palmer AG (2004) NMR characterization of the dynamics of biomacromolecules. Chem Rev 104:3623–3640

Pintacuda G, Keniry MA, Huber T, Park AY, Dixon NE, Otting G (2004a) Fast structure-based assignment of 15N HSQC spectra of selectively ^{15}N-labeled paramagnetic proteins. J Am Chem Soc 126:2963–2970

Pintacuda G, Moshref A, Leonchiks A, Sharipo A, Otting G (2004b) Site-specific labeling with a metal chelator for protein-structure refinement. J Biomol NMR 29:351–361

Prestegard JH, Bougault CM, Kishore AI (2004) Residual dipolar couplings in structure determination of biomolecules. Chem Rev 104:3519–3540

Rodriguez-Castaneda F, Haberz P, Leonov A, Griesinger C (2006) Pamagnetic tagging of diamagnetic proteins for solution NMR. Magn Reson Chem 44:S10–S16

Tang C, Iwahara J, Clore GM (2006) Visualization of transient encounter complexes in protein-protein association. Nature 444:383–386

Tolman JR, Flanagan JM, Kennesy MA, Prestegard JH (1995) Nuclear magnetic dipole interactions in field-oriented proteins – information for structure determination in solution. Proc Natl Acad Sci USA 92:9279–9283

Tolman JR, Flanagan JM, Kennesy MA, Prestegard JH (1997) NMR evidence for slow collective motions in cyanometmyoglobin. Nat Struct Biol 4:292–297

Volkov AN, Worrall JAR, Holtzmann E, Ubbink M (2006) Solution structure and dynamics of the complex between cytochrome c and cytochrome c peroxidase determined by paramagnetic NMR. Proc Natl Acad Sci 103:18945–18950

Wohnert J, Franz KJ, Nitz M, Imperiali B, Schwalbe H (2003) Protein alignment by a coexpressed lanthanide-binding tag for the measurement of residual dipolar couplings. J Am Chem Soc 125:13338–13339